Bremsstrahlung emission from quark stars

by

Jean-François Caron

BSc. (Honours) in Physics, The University of Calgary, June 2006

A THESIS SUBMITTED IN PARTIAL FULFILMENT OF
THE REQUIREMENTS FOR THE DEGREE OF

MASTER OF SCIENCE

in

The Faculty of Graduate Studies

(Physics)

THE UNIVERSITY OF BRITISH COLUMBIA

(Vancouver)

September, 2009

Abstract

We calculate numerically the emissivity and surface flux of electron-electron bremsstrahlung radiation from the surface of a bare quark star. The restricted electronic phase space due to the presence of an effective photon mass results in a strong suppression. The emissivity and surface flux are found to be substantially smaller than those found previous work [17], to the point where electron-positron pair production would remain the dominant radiation mechanism at all temperatures in the relativistic regime [35]. As a consequence, the distinct emission spectrum characteristic of electron-positron pair annihilation is a likely distinguishing characteristic of bare quark stars.

Table of Contents

List of Figures

Acknowledgements

I wish to thank my fellow graduate students for their support during the long years of work. Kory Stevens in particular helped elucidate the way to determine phase-space restrictions that are the core of this work. James Charbonneau had many valuable suggestions when I was stuck in a pointless calculation, and his advice in communicating with supervisors, publishers and the administration was invaluable. Various discussions with Kyle Lawson forced me to better understand the physics involved in my calculations, which I was sometimes taking for granted.

Part I

Thesis

1. Introduction

1.1 What is a Quark Star?

Quark stars are exotic theoretical objects that could result from a supernova explosion. When a normal with a large enough mass star runs out of nuclear fuel, the core contracts rapidly and the outer shell collapses onto it due to gravity. The resulting explosion is called a supernova. The supernova can eject much of the original star's mass. The remaining core of dense matter can take on several forms, depending on how much matter is left.

1.1.1 Neutron Stars

The first type of supernova remnant are neutron stars. In the cores the density will be so high that the nuclei start to touch and clump together. The star is no longer composed of nuclei or atoms, but of many neutrons and protons. The neutrons and protons are permeated by a cloud of ultra-relativistic (moving near the speed of light) and degenerate (energy levels are very tightly packed) electrons. Some protons and electrons merge to become neutrons because this relieves some of the "pressure" from the electrons. The end result is mostly made of neutrons, so we call this a neutron star. The gross structure of neutron stars is determined by the equilibrium point between the gravitational pull inward and the pressure of the neutrons outward.

1.1.2 Quark Stars

Remnants even heavier than neutron stars will have densities so high that the neutrons and protons may start to overlap. At this point the system is better described by a large mass of free quarks called quark matter. This exotic matter is not well understood and may exist in various configurations. It is thought that some neutron stars can contract as they cool, reaching the

densities required for a quark star to form. This process can be explosive [29] like the supernova that preceeded it and can further eject matter. As a result, quark stars can have masses similar to neutron stars.

Normal matter (protons and neutrons) is made up of only the two lighter quarks, called up and down. Because of the densities and pressures involved, the strange quark (the third lightest) is also produced. The strange quark is more massive than the up and down quarks which are nearly massless. The strange quark mass is therefore often an important parameter in models of quark matter. The three heavier quarks (charm, bottom, top) do not play a major role because their masses are much greater than even the strange quark. In fact it has been shown that quark stars at the extreme densities required to produce charm quarks (the lightest of the heavy three) are unstable [19].

It has long been conjectured [7, 9, 16, 26, 36] that quark matter could be the absolute ground state of the strong nuclear force. If this is the case, then quark matter would be more stable than iron, the most stable atomic nucleus. It is possible that quark matter is only stable at high pressures, in this case it would only be present in the cores of dense stars with an outer layer of normal matter [25]. These stars are called hybrid stars and have more in common with neutron stars because observations are mostly concerned with the outer layers of stars.

If the quark matter is stable without high pressures, it can exist without normal matter surrounding it [1]. This possibility of "bare" quark matter is very exciting, because it allows for nearly direct observations about the strong nuclear force. These observations would also yield information about the state of matter at high *densities* while nearly all high-energy experiments on earth yield information about matter at high *temperatures*.

The exact behavior of quark matter is not well understood. A plethora of models exist describing the microscopic details and thermodynamic properties [4]. Most models involve some kind of colour-superconductivity and a condensed phase where quarks form pairs. The pairing mechanisms are not perfect however, because the strange quark has a mass very different from the up and down quarks. If their masses were exactly equal, there would be equal quantities of all three quarks and their electromagnetic charges (2/3, $-1/3$, $-1/3$ for the up, down, and strange quarks, respectively) would exactly cancel out. The strange quark has a higher mass, so it "costs" more energy to produce and there are fewer present. The result is a net positive charge because the up and down quarks are found in equal numbers [1, 4, 25].

The gross structure of quark stars is determined by the equilibrium point between the pull of the strong interaction inward and the pressure of the quarks themselves. Quark stars are so-called "self-bound" objects, meaning that the force pulling the matter in is not gravity, as is the case with all other stars, but the strong nuclear force. All other stars have a certain minimum mass, because as the mass decreases, the gravitational force binding the matter into the star also decreases. At some point, the fine balance between the gravitational force and the outward-pushing pressure would not be able to be achieved, and the star would lose matter in a process similar to boiling or evaporation. Being self-bound, quark stars of arbitrarily small masses can be obtained, because decreasing the mass of a quark star does not diminish the strength of the strong nuclear force. Gravity is not required for the stability of quark stars, but it still plays an important role in the dynamics, especially for those quark stars whose masses are similar to neutron stars [15].

Quark stars are expected to have a crust of normal matter at formation. There is a calculated maximum mass for this crust [13], but this would be enough to completely obscure the quark surface underneath, making observation difficult. Fortunately quark stars end up shedding their crusts soon after formation because when quark stars are formed, they are very hot ($T \sim 10^{11}\,\mathrm{K}$) [14]. At these high temperatures, the quark matter is transparent to neutrinos and neutrino cooling dominates. The neutrinos push any crustal matter away from the star [37]. There may be arrangements where a crust would re-form after cooling, e.g. if there is a companion star from which matter is accreting [1], but these would be special cases and are not considered here.

The boundary between quark matter and regular matter is expected to be very sharp. The transition occurs in a thickness of $\sim 10^{-15}\,\mathrm{m}$, the length scale of the strong interaction. This sharp transition along with the lack of a crust leads to an extremely strong electric field at the quark surface since the quark matter is positively charged. This electric field will attract electrons until the total charge is equilibrated at zero. The quark matter is bound by the strong interaction while the electrons are only attracted by the much weaker electromagnetic force. As a result, the electrons pool around the quark matter but also extend out into space. The part of the electron cloud outside of the quark matter is called the "electrosphere" analogously to the atmosphere on planets [1].

There are some studies which indicate that quark stars may have much thicker electrospheres at an overall lower density [18], however these mod-

els have more constrained parameters. They are less likely to be realized in nature [3] and the modifications occur mostly in the non-relativistic regime where our model is inadequate. We will not consider these "thick electrosphere" models in this work.

1.1.3 Black Holes and Analogies

The heaviest stars that go supernova will collapse into black holes. Imagine neutron star cores as being giant atomic nuclei composed of protons and neutrons. Quark star cores can then be thought of as giant neutrons or protons composed of many quarks. Black holes have no everyday analogy. Although quark matter may be the absolute ground state of the strong nuclear force, at sufficient densities gravity takes over again and the matter collapses into a black hole.

1.2 Why Study Quark Stars?

Quark stars are very interesting objects because their properties are so extreme. Typical temperatures are 10^9 K [34] and densities are above nuclear saturation ($10^{18}\,\mathrm{kg/m^3}$). Macroscopic stable objects with these properties could never be achieved in a laboratory, but understanding them can give us insight into the fundamental forces and particles of nature. All four forces of nature are involved in the dynamics: the familiar electromagnetic and gravitational forces, and the two short-range nuclear forces.

As mentioned in Section 1.1.2, the physics involved in quark stars is high energy, but the high energy is attained through high *densities*. Most high-energy experiments performed in laboratories involve high *temperatures*. There are many parallels between the two, for example the charge-separation effect [21, 22] (a high-temperature phenomenon) seen at RHIC may be analogous to certain non-dissipative currents in dense matter [8, 27]. Observation of quark stars would give information about the high density behavior of strongly coupled matter.

Quark matter is also the key component the dark matter candidates called "strangelets" [25, 28, 36, 38]. These are essentially very-low-mass quark stars which are composed of anti-quarks. Because they are very small and much colder, many properties of strangelets need to be considered in the relativistic or non-relativistic regime [23]. Extending the current work on quark stars to

include these regimes would have direct applications to strangelets.

The strange matter hypothesis has not been confirmed. It leads to many beautiful results in physics, one of which is the existence of quark stars. The unambiguous observation of a quark star would settle the issue of the stability of strange matter. More detailed observations would also allow for better understanding of the strong nuclear force.

1.2.1 Observation

Black holes have been observed unambiguously. Neutron stars are generally believed to be pulsars in astronomy [33]. Quark stars have not yet been unambiguously observed. However, quark stars and neutron stars are thought to look very similar when observed astronomically [15]. For example they have overlapping ranges of masses and maximal spin frequency. Thus many of our pulsar observations could in principle be either kind of object. There are some pulsars that are clearly not quark stars, but there are none so far that are clearly not neutron stars.

Because they are self-bound, quark stars could have much smaller masses than those allowed for neutron stars. Thus an observation of a very low mass pulsar would be strong evidence for the existence of quark stars and the strange matter hypothesis in general [1, 15]. Unfortunately such low mass stars would be very dim and hard to find; mass measurements are also very difficult to obtain.

Normal stars are limited in their luminosity by the so-called Eddington limit. This upper limit on luminosity is when the pressure due to to the outgoing radiation equals the gravitational pull on the upper layers of matter in the star. If the luminosity is beyond the Eddington limit, the star would quickly blow away its outer layers and lose mass dramatically. Quarks stars are self-bound however, so even if the radiation pressure is strong enough to blow away gravitationally-bound matter, it would not eject quark matter because it is bound by the much stronger nuclear force. As a result, quark stars may have "super-Eddington" luminosities for extended periods of time, up to months [30]. Observation of objects with long-term intense emission would be a key signature of quark stars.

1.3 Radiation Processes

There are still no good properties that can be used to distinguish quark stars from neutron stars. Significant radiation processes are of obvious interest for this purpose. The processes of interest for quark stars are equilibrium photons, electron-positron pair production with subsequent annihilation [30, 34, 35], and electron-electron bremsstrahlung [17]. All of these occur in the electrosphere. Radiation from the quark core is not significant because the densities are so high that nearly all radiation is re-scattered before it can escape [1]. In the electrosphere, the high density still prevents low-frequency photons from escaping, but photons above a certain frequency are allowed to propagate unhindered. This certain frequency is called the *plasma frequency* (ω_p) and can be thought of as arising from an effective photon mass [31]. Just as electrons cannot have energies less than 511 keV because of their mass, photons in the electrosphere cannot have a frequency less than the plasma frequency.

The plasma frequency depends on the chemical potential of the electrons and on the temperature. Further from the crust of the quark star, the density of electrons decreases (see Figure 1.4), and so does the plasma frequency. This means that a photon emitted with an energy above ω_p will be able to escape the star as long as it was emitted "outwards". Photons directed inward will encounter a denser region and will then be re-absorbed. The plasma frequency formula is given in Eq. (2.2).

In reality, photons with energy less than the plasma frequency can still propagate, but they are extremely attenuated. A sub-ω_p photon can travel a small distance into a neighbouring region without being fully extinguished in a process similar to tunnelling in quantum mechanics. If the neighbouring region has a lower plasma frequency than the photon's energy, it can continue propagating freely. This process is most likely to occur where the plasma frequency changes most rapidly with distance, so that the two adjacent regions may have very different plasma frequencies. The region with the fastest-varying plasma frequency is near the quark surface, but this is also where the plasma frequency is highest. Thus this process is not expected to significantly affect the primary radiation mechanisms described below.

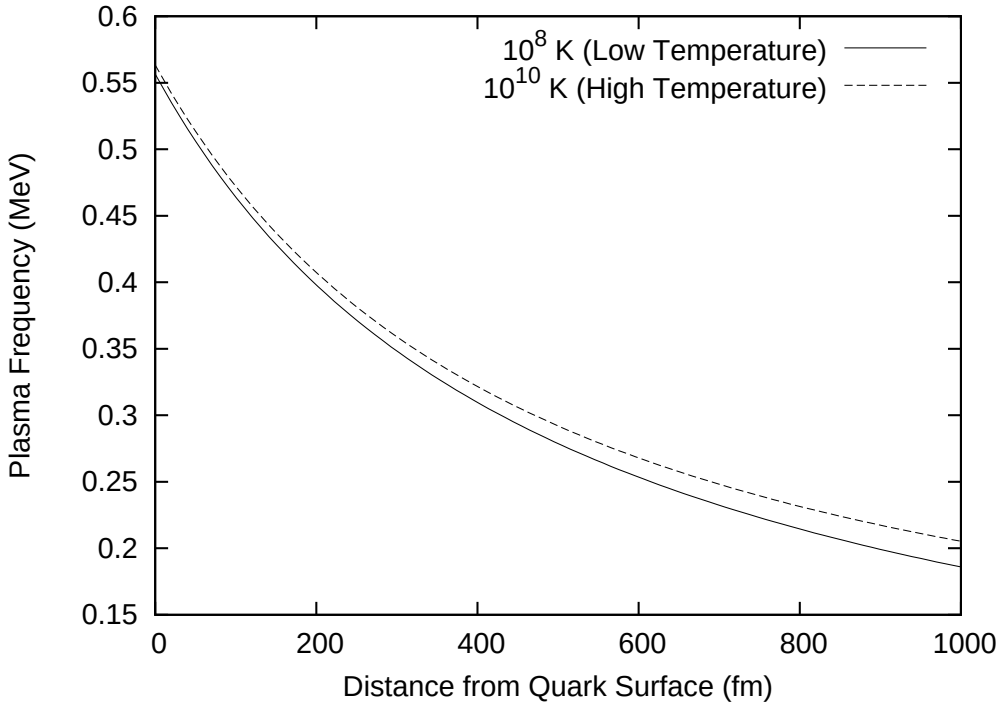

Figure 1.1: Plasma frequency as a function of distance from the quark surface at two temperatures. We have used a chemical potential profile described later in Section 1.5.

1.3.1 Equilibrium Photons

Quark matter is bound by the strong nuclear force, but quarks also have an electromagnetic charge. The motions of these charges results in photons being emitted. In dense quark matter, the quarks exist in equilibrium with the photons, where the rate of emission equals the rate of absorption. At sufficiently high temperatures, the photons will have a high enough energy to escape the quark matter. The strength of this radiation is enough to dwarf all other processes, but only at very high temperatures $T > 5 \times 10^{10}\,\mathrm{K}$[34].

1.3.2 Electron-Positron Pair Production

Electron-positron pair production (e^+e^-) results from the strong electric field present in the electrosphere as described in Section 1.1.2. The quark core has a positive charge, but has a hard edge which results in a very large electric field. When the energy density of the electric field becomes comparable to the mass of the electron, it is energetically preferable to spontaneously create electrons and positrons in pairs in order to lower the electric field. This process is known as the Schwinger mechanism [32]. At zero temperature, there are no available energy states in which to place new electrons. At finite temperature however, there are unoccupied states with energies near the chemical potential (see Section 1.4). As a result, this process is strongly temperature-dependent [35].

The electrons and positrons produced will recombine and annihilate into photons. The radiation produced has a distinct energy spectrum that does not occur in neutron stars [35]. The spectrum is also dominated by higher energy photons, so the presence of a plasma frequency as mentioned in Section 1.3 is less relevant for this process. Most photons have energies above the plasma frequency and thus are able to propagate freely. It was found that this process is dominant for temperatures $5 \times 10^{10}K > T > 8 \times 10^{8}K$ [30]. For extremely low temperatures $T < 8 \times 10^{8}K$, results indicated that $e^+e^-$and equilibrium photons would also dominate, although the results were more uncertain [34].

1.3.3 Electron-Electron Bremsstrahlung

Bremsstrahlung (literally "braking radiation") occurs when a charged particle is accelerated or decelerated. The faster the change, the more intense

the radiation. In the case of the electrosphere of the quark star, electrons are "braking" against other electrons, losing energy in the form of radiation. In the ultra-relativistic approximation, the energy spectrum is broad and includes photons of arbitrarily low energy (see Figure 1.2). Indeed most of the photons emitted will be on the low-energy side, so the plasma frequency limit is quite important.

Contrary to the result in Ref. [30], another study [17] found that electron-electron bremsstrahlung and not $e^+e^-$is the dominant process for temperatures $10^8\,\mathrm{K} > T > 10^9\,\mathrm{K}$. Thus very hot stars would radiate equilibrium photons, moderately hot stars would radiate photons from electron-positron annihilation, while cooler stars (the majority) would radiate photons from electron-electron bremsstrahlung. Unfortunately the authors of [17] incorrectly neglected some aspects of the high density environment. The aim of this work is to settle the question regarding which process is dominant in the contested temperature range.

1.4 Previous Work

Jaikumar et al. [17] attempted to obtain an analytic result, expressible as a simple function that can be easily used for other purposes. In order to obtain this, they used Low's theorem for the emission of low-energy photons [24]. Low's theorem states that calculating the full cross-section for bremsstrahlung is unnecessary when only considering photon energies below a certain value. Because bremsstrahlung is known to be dominated by lower energy photons, this seems like a valid technique. The only cross-section needed in this case is the electron-electron elastic scattering (Møller scattering) which is much simpler than the full electron-electron bremsstrahlung cross-section. This much simpler expression can yield analytic results.

The authors partially considered the effect of the high degeneracy of electrons. Specifically, they used the plasma frequency as a minimum photon energy. Unfortunately because they were using Low's theorem for low-energy photons, the energy range of photons was restricted to a narrow range between the plasma frequency and that allowed by Low's theorem. In our work we use an ultra-relativistic cross-section for electron-electron bremsstrahlung [2] which is valid for all photon energies up to $\omega - \omega_{max} \ll m_e$ (see Section 2.4). Although some photons are neglected, we include a much greater range of photon energies than the authors of Ref. [17]. The neglected photons could

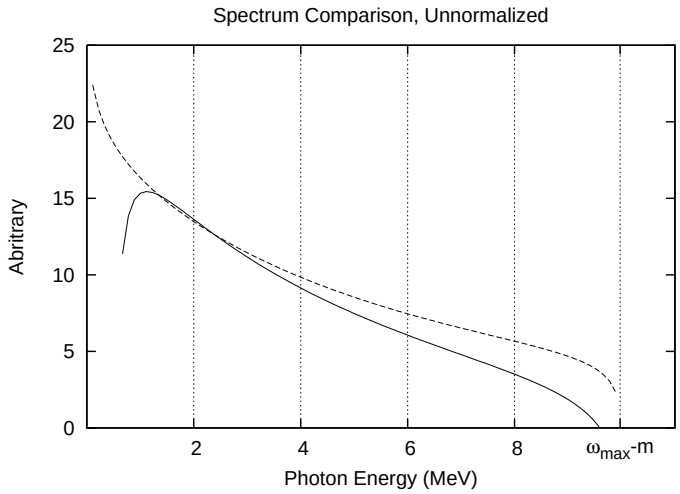

Figure 1.2: Comparison plot of the electron-electron bremsstrahlung spectrum. The solid line is from Jaikumar et al. [17]. The dashed line is from the cross-section (see Eq. 2.36) used in this work [5].

in principle be accounted for, however the cross-section for emission of higher energy photons is much smaller, so this would be a small contribution.

Further, the energy of the emitted photon is required by Low's theorem to be much lower than all other energy scales in the process. This is easy to achieve with ultra-relativistic electrons, but the scattering process also involves a virtual photon exchange between the electrons which is not necessarily of low energy. For Low's theorem to be valid, the authors had to artificially restrict the electron scattering angles in order for this virtual photon to have valid energies. Due to these artificial limits, the authors eventually arrive at a cross-section expression with an overall factor of $1/\epsilon^2$ (see Eq. (36) from [17]) where ϵ is the incoming electron energy. When the full allowed kinematic phase space is included, there is no such term and the relevant behavior is $1/m^2$. Typical electron energies are $\epsilon \sim \mu$ so our results have an overall enhancement above that used by Jaikumar et al. of μ^2/m^2 or about a factor of 10^2.

Finally and most importantly, although the effect of the plasma frequency on the emitted photon was included, the effect on the allowed energies of the electrons was ignored. The electrons in the electrosphere are highly degen-

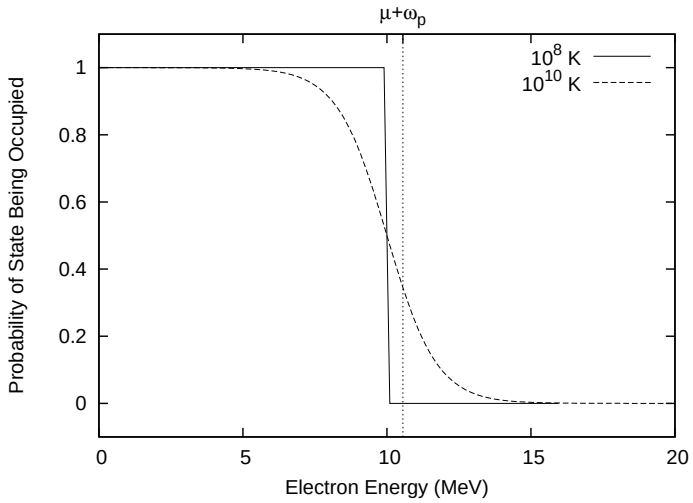

Figure 1.3: The Fermi function $1/(1 + exp(\epsilon - \mu/T))$ describes the probability of energy states being occupied. At low temperatures, the system is strongly degenerate so that almost all energies below the chemical potential are occupied. At high temperatures there are some states above and below the chemical potential that are open. In this example the chemical potential is 10 MeV. Electrons whose energies are to the right of the line at $\mu + \omega_p$ are those which are likely to participate in bremsstrahlung.

erate, meaning that their energies are all very close to each other. Electrons are fermions, which means that no two electrons can be in the same quantum state. Since the energies are all very closely packed together, there is little "room" to put in new electrons. This is only true up to a certain point. Once a high enough energy is reached (called the chemical potential), the energy levels are almost all vacant and there is lots of room for electrons. This means that electrons that participate in bremsstrahlung are likely to have energies below the chemical potential (this is where almost all the electrons live). In emitting radiation, the electrons will lose energy. Unfortunately the lower energy states where they should now live are already occupied by other electrons! If the electrons have "nowhere to go" after emitting radiation, they simply won't emit radiation. This phenomenon is called "Pauli suppression" because the statement that fermions cannot occupy the same energy levels is the Pauli exclusion principle.

Because of Pauli suppression, most of the electrons that could emit radiation are those whose energies are near or above the chemical potential. These can lose a little bit of energy but still have an empty energy state in which to end up. Unfortunately for the electrons, there is another effect - the plasma frequency - that requires the emitted photon to be above a certain energy. Thus even electrons near or slightly above the chemical potential won't be able to emit radiation, because they would lose too much energy and end up deep below the chemical potential. The end result is that only those electrons who have energies well above the chemical potential can radiate. These electrons are rare indeed, because the chemical potential is the point at which the energy levels change from being mostly full to mostly empty.

The resulting suppression from the plasma frequency is severe. To illustrate how the suppression comes about, consider the following example which integrates a single particle momentum over a Fermi function with the additional restriction of a minimum energy. This is a typical integral in thermal quantum field theory, where integrals over energy include a Fermi function to account for the fact that not all energy states are available. Please refer to Appendix A for an explanation of the units and mathematical notation used. The minimum energy is represented by a Theta function (see Eq. 2.3).

$$\int_0^\infty \frac{d^3p}{(2\pi)^3} \frac{2}{e^{(\epsilon-\mu)/T}+1} \Theta(\epsilon-\mu-\omega_p). \tag{1.1}$$

Changing variables to a dimensionless excitation energy parameter

$$x = (\epsilon-\mu)/T \tag{1.2}$$

and taking the ultra-relativistic and degenerate approximation $|\vec{p}\,| = \epsilon = \mu$ for the polynomial p^2 term, we obtain

$$\frac{\mu^2 T}{\pi^2} \int_{\omega_p/T}^\infty \frac{dx}{e^x+1}. \tag{1.3}$$

Since $\omega_p > T$, we have $e^x \gg 1$ for all x in the integration region. The result is

$$\frac{\mu^2 T}{\pi^2} e^{-\omega_p/T} \tag{1.4}$$

whereas the result without ω_p is

$$\frac{\mu^2 T}{\pi^2} \ln 2. \tag{1.5}$$

This one-particle phase volume example illustrates how the suppression comes about. In this work the calculation is done numerically so a similar analytic expression for the suppression of bremsstrahlung when multiple particles participate cannot be given. However such an exponential suppression will be always present when the restriction $\omega > \omega_p$ is imposed.

The previous work ignored these effects and only considered the role of the plasma frequency on limiting the photon energies. Limiting the photon energies however has consequences for the electron energies which lead to the severe suppression of the form $\exp(\omega_p/T)$. This suppression is very strong because in nearly all regions of the electrosphere $\omega_p \gg T$. The only exception is at very large temperatures above a few $10^{10}\,\mathrm{K}$ where $\mu \sim T$ so that the electrons are less degenerate and the Pauli suppression is almost gone. In this case our inclusion of the full photon energy range and allowed kinematic phase space (because we do not use Low's theorem) actually enhances the bremsstrahlung radiation. At these temperatures however, the emission is dominated by equilibrium photons [34] so the exact strength of electron-electron bremsstrahlung radiation — even to a few orders of magnitude — is less relevant.

The calculation by Jaikumar et al. also considered the inclusion of the Landau-Pomeranchuk-Migdal (LPM) effect [6]. The LPM effect encompasses multiple scattering of radiation in high-density matter. This is most important when the wavelength of the radiation is comparable to or longer than the spacing of scattering centers. The result is suppressed emission of low-energy photons. We do not explicitly include the LPM effect in this work because the suppression by the phase-space constraints is strong enough to make electron-electron bremsstrahlung negligible. Inclusion of the LPM effect would simply suppress it further. More importantly, this suppression is expected to be numerically similar as discussed previously [17]. It could therefore be implemented if it is needed.

1.5 Our Model

Our model of the electrosphere has a uniform temperature because the strongly degenerate electrons are easily able to transport heat [10]. The radiation is calculated at various temperatures from $10^8\,\mathrm{K}$ to $10^{10}\,\mathrm{K}$. We take the chemical potential (related to the density) of the electrons at the surface of the quark matter to be $\mu_0 = 10\,\mathrm{MeV}$ corresponding to a density of $\sim 10^9\,\mathrm{kg/m^3}$

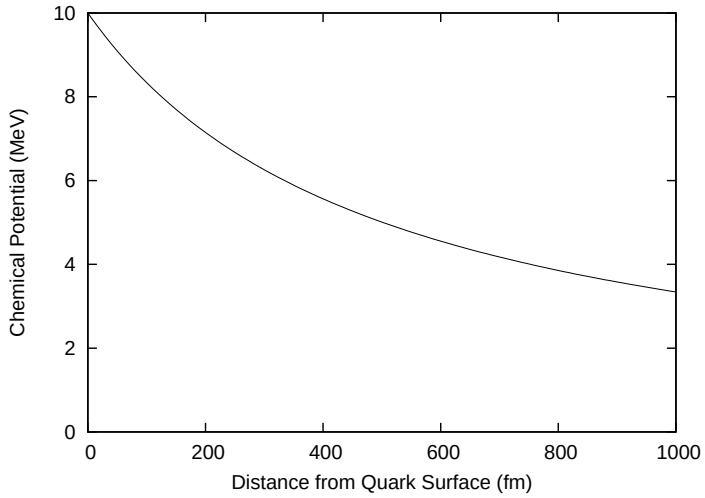

Figure 1.4: Chemical potential profile. The non-relativistic regime occurs when $\mu \sim m = 0.511\,\mathrm{MeV}$. The non-degenerate regime occurs when $\mu \sim T \approx 0.1\,\mathrm{MeV}$.

at zero temperature. As one moves further away from the surface, the chemical potential decreases rapidly. At far enough distances, the electrons will no longer be ultra-relativistic and some of our approximations will no longer be appropriate. Luckily at these lower chemical potentials, the density of electrons is also much lower and little emissivity would be seen here. The radiation from these far regions could be included, but it is expected to be a small contribution to the overall radiation. The work by Jaikumar et al. restricted itself to distances less than 1000 fm from the surface so we duplicate this artificial boundary for ease of comparison. The chemical potential profile is [20]

$$\mu(z) = \frac{\mu_0}{1 + z/H} \tag{1.6}$$

where

$$H = \frac{1}{\mu_0}\sqrt{\frac{3\pi}{2\alpha}}. \tag{1.7}$$

2. Calculation Details

2.1 Emissivity

A quantity of interest in comparing emission mechanisms is the *emissivity*. The emissivity is the amount of energy emitted per time per volume of electrons. In common units emissivity would have dimensions of watts per cubic metre, but here it is expressed as eV^5. It is given by the following integral:

$$\frac{1}{2}\int \frac{d^3p_1}{(2\pi)^3}\frac{d^3p_2}{(2\pi)^3}F(\epsilon_1,\epsilon_2,\cos\theta_{12})\Theta(\epsilon-\omega_p-2\mu-2m)\Theta(\epsilon_1-\mu-m)\Theta(\epsilon_2-\mu-m) \tag{2.1}$$

where ϵ_1 and ϵ_2 are the energies of the two incoming electrons and $\vec{p}$'s their momenta. $\cos\theta_{12}$ is the scattering angle of the final electrons. The overall $1/2$ in front is because only electrons emitted towards the exterior of the electrosphere will escape. Those directed inwards will encounter a region where they can no longer propagate, either a denser region of the electrosphere or the quark matter itself. The factor is only $1/2$ because we use a "plane-parallel" approximation. The electrosphere is very close to the quark surface and is very thin $\sim 1000\,\mathrm{fm}$ while quark stars with typical masses are on the order of kilometres in radius. This makes it reasonable to treat the quark surface as an infinite wall on one side, with the electrosphere extending into space on the other side. The plasma frequency is [31]

$$\omega_p = \sqrt{\frac{4\alpha\mu^2}{3\pi}+\frac{4\alpha\pi T^2}{9}} \tag{2.2}$$

in terms of the electron chemical potential μ and the temperature T. This is only valid in the ultra-relativistic case where the chemical potential is much greater than the electron mass. It most cases $T \ll \mu$, so $\omega_p \approx \mu/20$.

The Θ-functions are Heaviside functions used to denote limits of integration. A Heaviside function is simply a step function from zero to one at zero.

More formally:

$$\Theta(x) = \begin{cases} 0, & x \leq 0 \\ 1, & x > 0 \end{cases} \tag{2.3}$$

Essentially $\Theta(x-a)$ is notation meaning "x must be greater than a". The total energy in the centre of mass frame is

$$\begin{aligned} \epsilon &= \sqrt{(\epsilon_1+\epsilon_2)^2 - (\vec{p}_1+\vec{p}_2)^2} & (2.4) \\ &= \sqrt{2\epsilon_1\epsilon_2 + 2m^2 - 2|\vec{p}_1||\vec{p}_2|\cos\theta_{12}}, & (2.5) \end{aligned}$$

it is expressed as a kinematic invariant so that we may use it in abritrary frames of reference. The Θ-function containing this term is the core of the suppression. ϵ must be large enough so that the emitted photon has energy above the plasma frequency, but it must also be large enough so that the outgoing electrons have empty energy levels available.

$$F(\epsilon_1, \epsilon_2, \cos\theta_{12}) = 2n(\epsilon_1)2n(\epsilon_2)(2\tilde{n}(\mathcal{E}))^2 \int_{\omega_p}^{\omega_{max}} \omega \left(\frac{d\sigma}{d\omega}\right) d\omega \tag{2.6}$$

combines initial state Fermi functions $n(\epsilon_i)$, an effective final state degeneracy factor $\tilde{n}(\mathcal{E})$ (see Eq. (2.38)) and the first moment of the electron-electron bremsstrahlung cross-section. Including instead the zeroth moment of the cross-section (without the extra ω in the integral) would yield a rate (number of photons emitted per time per volume) rather than an emissivity. The factors of 2 account for the fact that electrons have two spin states that may be occupied at each energy.

2.2 Phase-Space Constraints

The Θ-functions in (2.1) are in terms of electron energies ϵ, but the integrals are over electron momentum $\vec{p}$. In this section we rearrange the Θ-functions to give explicit constraints on the energies and scattering angles of the electrons. The range over which all variables are integrated is called the phase space.

2.2.1 Angular Restriction

The Θ-function containing ϵ can be used as a restriction on the angle between incoming electrons:

$$\underbrace{\sqrt{2\epsilon_1\epsilon_2 + 2m^2 - 2|\vec{p}_1||\vec{p}_2|\cos\theta_{12}}}_{>0} > \underbrace{\omega_p + 2\mu + 2m}_{>0} \tag{2.7}$$

$$\epsilon_1\epsilon_2 + 2m^2 - 2|\vec{p}_1||\vec{p}_2|\cos\theta_{12} > (\omega_p + 2\mu + 2m)^2 \tag{2.8}$$

$$\cos\theta_{12} > \frac{\frac{1}{2}(\omega_p+2\mu+2m)^2 - m^2 - \epsilon_1\epsilon_2}{|\vec{p}_1||\vec{p}_2|}. \tag{2.9}$$

We can square the inequality to get rid of the square root sign because both quantities are positive. A common quantity in these calculations is

$$\Delta = m^2 - \frac{1}{2}(\omega_p + 2\mu + 2m)^2. \tag{2.10}$$

So the angular integration is restricted to

$$\cos\theta_{12} > \frac{-\Delta - \epsilon_1\epsilon_2}{|\vec{p}_1||\vec{p}_2|}. \tag{2.11}$$

The value of Δ depends on the chemical potential μ and the temperature T. For typical $T \sim 1$ MeV and $\mu \sim 10$ MeV, we have $\Delta \sim -233$ MeV^2. Δ is always a negative quantity with dimension eV^2, it decreases quadratically with μ and approximately linearly with T for our parameter ranges. At $T = 0$, $\mu = 0$, we have the maximum value of $\Delta = -m^2$.

2.2.2 Energy Restrictions

The electron energies are restricted by the two $\Theta(\epsilon_i - \mu - m)$ functions to be greater than $\mu + m$. This is because our cross section is taken from Ref. [2], where the final electron energies were already integrated. This integration was done at zero temperature and chemical potential. Done properly, the final states would have been integrated over inverse Fermi functions. Restricting the initial energies to be above the chemical potential is an approximate accounting for this, but it overstates the final state degeneracy slightly. Both energies are constrained by $\epsilon_i > \mu - m$ where $i = 1, 2$.

In addition to the above constraints, the angular restriction (2.11) also affects the electron energies. We illustrate how some electron energies are not valid based on the need for scattering angles to be real. For real angles,

$1 > \cos\theta_{12} > -1$. Is this compatible with the condition (2.11) above? At high energies, $\epsilon_1,\ \epsilon_2 \to \infty$ the condition becomes $\cos\theta_{12} > -1$ which is consistent.

Unfortunately as $\epsilon_1,\ \epsilon_2 \to \mu + m$, the condition yields $\cos\theta_{12} \gtrsim 1.1$ for typical μ and T. Thus, simply using (2.11) as a condition on $\cos\theta_{12}$ is not enough, we seem to have "lost" some of the information contained in the Θ-function when squaring. To reinforce the constraint (and thus keep scattering angles real), we impose that the quantity which must be less than $\cos\theta_{12}$ be less than 1:

$$\frac{-\epsilon_1\epsilon_2 - \Delta}{|\vec{p}_1||\vec{p}_2|} < 1. \tag{2.12}$$

Rearranging and substituting $|\vec{p}\,| = \sqrt{\epsilon^2 - m^2}$:

$$\epsilon_1\epsilon_2 + \Delta > -\sqrt{\epsilon_1^2 - m^2}\sqrt{\epsilon_2^2 - m^2}. \tag{2.13}$$

The right hand side of this equation is always negative, while the left hand side can change sign. At high energies, the left hand side is positive, but at low energies it can be negative since Δ has a negative value. We would like to re-arrange this inequality to yield a restriction on ϵ_1 as a function of ϵ_2, but it must be squared. Since one side does not have a definite sign, two cases arise:

Case 1: $\epsilon_1\epsilon_2 + \Delta < 0$

This case arises at the low-energy part of the integration when ϵ_1 and ϵ_2 are both near $\mu + m$. In this region, both sides of the equation are negative, so squaring each side reverses the inequality sign:

$$\begin{aligned}
(\epsilon_1\epsilon_2 + \Delta)^2 &< (\epsilon_1^2 - m^2)(\epsilon_2^2 - m^2) \\
\epsilon_1^2\epsilon_2^2 + 2\epsilon_1\epsilon_2\Delta + \Delta^2 &< \epsilon_1^2(\epsilon_2^2 - m^2) - m^2(\epsilon_2^2 - m^2) \\
\epsilon_1^2 m^2 + 2\epsilon_1\epsilon_2\Delta + (\Delta^2 + m^2 \underbrace{(\epsilon_2^2 - m^2)}_{|\vec{p}_2|^2}) &< 0.
\end{aligned} \tag{2.14}$$

This is factored using the quadratic equation.

$$\begin{aligned}\epsilon_\pm &= \frac{-\Delta\epsilon_2 \pm \sqrt{\Delta^2\epsilon_2^2 - m^2(\Delta^2 + m^2|\vec{p}_2|^2)}}{m^2} \\ &= \frac{1}{m^2}\left(-\Delta\epsilon_2 \pm |\vec{p}_2|\sqrt{\Delta^2 - m^4}\right) \\ &= \frac{-\Delta\epsilon_2}{m^2}\left(1 \pm \sqrt{1 - \frac{m^2}{\epsilon_2^2}}\sqrt{1 - \frac{m^4}{\Delta^2}}\right),\end{aligned} \tag{2.15}$$

where we made use of $|\Delta| = -\Delta$ and $\frac{|\vec{p}_2|}{\epsilon_2} = \sqrt{1 - \frac{m^2}{\epsilon_2^2}}$.

Note that since Δ is negative, then ϵ_+ is always positive. We know that $m^2 < \epsilon_2^2$ from the $\Theta(\epsilon_2 - \mu - m)$ term in the original integral. We also know that $m^4 \leq \Delta^2$ for all values of μ and T. From these we can then tell that ϵ_- is also positive, since the square root terms will each be less than one. The condition (2.13) in factored form is

$$(\epsilon_1 - \epsilon_+)(\epsilon_1 - \epsilon_-) < 0. \tag{2.16}$$

Thus we reach the condition that either $\epsilon_1 < \epsilon_+$ or $\epsilon_1 < \epsilon_-$ but not both (exclusive or). However from the expression for $\epsilon_\pm$, we clearly see that $\epsilon_+ > \epsilon_-$. Thus the condition becomes:

$$\epsilon_+ > \epsilon_1 > \epsilon_-. \tag{2.17}$$

Case 2: $\epsilon_1\epsilon_2 + \Delta > 0$

This case occurs at high energies, specifically at a large product of ϵ_1 and ϵ_2. The criterion for this case is already more restrictive than Eq. (2.13). So we use

$$\begin{aligned}\epsilon_1\epsilon_2 + \Delta &> 0 \\ \epsilon_1 &> \frac{-\Delta}{\epsilon_2}.\end{aligned} \tag{2.18}$$

Examining this condition and the criterion for this case, we see that they are identical. So in the case of $\epsilon_1\epsilon_2 + \Delta > 0$, there are actually no extra restrictions.

The Boundary Between Cases 1 and 2

The point where we switch from Case 1 to Case 2 occurs when $\epsilon_1\epsilon_2 + \Delta = 0$. In terms of ϵ_2 it occurs when:

$$\epsilon_2 = \frac{-\Delta}{\epsilon_1}. \tag{2.19}$$

The energies are also restricted to each be above $\mu+m$. The line $\epsilon_1\epsilon_2+\Delta = 0$ crosses $\epsilon_1 = \mu + m$ at $\epsilon_2 = -\Delta/(\mu + m)$ and similarly for $\epsilon_1 \leftrightarrow \epsilon_2$.

2.2.3 Paranoia Creeping In

If we let only one of the energies grow while keeping the other constant, there could arise further problems. For example as $\epsilon_1 \to \infty$ we can see that the condition (2.11) becomes $\cos\theta_{12} > \frac{-\epsilon_2}{\sqrt{\epsilon_2^2-m^2}}$ which is less than -1. Again we will restrict the energies so that this does not occur. Specifically we wish to only include energies where

$$\frac{-\Delta - \epsilon_1\epsilon_2}{|\vec{p}_1||\vec{p}_2|} > -1. \tag{2.20}$$

Again, one side of this inequality might be positive or negative, so we have to deal with each case separately:

Case 1: $-\Delta - \epsilon_1\epsilon_2 < 0$

Both sides of the inequality are negative in this case, so we square each side and reverse the inequality. Re-arranging yields

$$(\Delta + \epsilon_1\epsilon_2)^2 < (\epsilon_1^2 - m^2)(\epsilon_2^2 - m^2). \tag{2.21}$$

This is the exact same expression as (2.14) so the result is the same:

$$\epsilon_+ > \epsilon_1 > \epsilon_-. \tag{2.22}$$

This is not surprising, since the two conditions are effectively $-x < 1$ and $x > -1$.

Case 2: $-\Delta - \epsilon_1\epsilon_2 > 0$

The condition for this case is the same as in section (2.2.2). So again in this case we obtain

$$\epsilon_1 > \frac{-\Delta}{\epsilon_2} \tag{2.23}$$

2.2.4 Overlapping Restrictions

The restriction (2.17) seems odd. Why should there be an upper bound on the energy? It would make sense if $\epsilon_- = -\Delta/\epsilon_2$, then this would merely be the boundary between Cases 1 and 2, but they are in fact not equal. Luckily the upper bound $\epsilon_+ > \epsilon_1$ can be shown to be irrelevant for the entirety of Case 1. Specifically, we show that $\epsilon_+ > \epsilon_1$ is always satisfied in Case 1 (where $\epsilon_1 < -\Delta\epsilon_2$) because $-\Delta/\epsilon_2 < \epsilon_+$. Starting from expression (2.15) for ϵ_+:

$$\begin{aligned}
\epsilon_+ &> \frac{-\Delta}{\epsilon_2} \\
\frac{-\Delta\epsilon_2}{m^2}\left(1 + \sqrt{1-\frac{m^2}{\epsilon_2^2}}\sqrt{1-\frac{m^4}{\Delta^2}}\right) &> \frac{-\Delta}{\epsilon_2} \\
\left(\sqrt{1-\frac{m^2}{\epsilon_2^2}}\sqrt{1-\frac{m^4}{\Delta^2}}\right) &> \underbrace{\frac{m^2}{\epsilon_2^2} - 1}_{<0} \\
\left(\sqrt{1-\frac{m^2}{\epsilon_2^2}}\sqrt{1-\frac{m^4}{\Delta^2}}\right) &> 0 \\
\left(1-\frac{m^2}{\epsilon_2^2}\right) &> 0 \\
\epsilon_2^2 &> m^2
\end{aligned} \tag{2.24}$$

The final expression is clearly always satisfied, thus the restriction of being within Case 1 already satisfies $\epsilon_+ > \epsilon_1$.

The lower bound of (2.17) is not artificial in this way, as it can be shown that $\epsilon_- > \mu + m$ somewhere within Case 1, so that some part of Case 1 is

excluded. We show this to be the case at a specific value of $\epsilon_2 = \mu + m$.

$$\begin{aligned}
\epsilon_-|_{\epsilon_2=\mu+m} &> \mu + m \\
\frac{-\Delta(\mu+m)}{m^2}\left(1 - \sqrt{1-\frac{m^2}{(\mu+m)^2}}\sqrt{1-\frac{m^4}{\Delta^2}}\right) &> \mu + m \\
\left(1 - \sqrt{1-\frac{m^2}{(\mu+m)^2}}\sqrt{1-\frac{m^4}{\Delta^2}}\right) &> \frac{m^2}{-\Delta} \\
-\Delta\left(1 - \frac{m^2}{-\Delta}\right) &> -\Delta\sqrt{1-\frac{m^2}{(\mu+m)^2}}\sqrt{1-\frac{m^4}{\Delta^2}} \\
-\Delta - m^2 &> \sqrt{\Delta^2 - m^4}\sqrt{1-\frac{m^2}{(\mu+m)^2}}
\end{aligned}$$

We can square this because again both sides are positive.

$$\begin{aligned}
\Delta^2 + 2\Delta m^2 + m^4 &> \Delta^2 - \frac{\Delta^2 m^2}{(\mu+m)^2} - m^4 + \frac{m^6}{(\mu+m)^2} \\
2m^2(\Delta + m^2) &> \frac{m^2}{(\mu+m)^2}(-\Delta^2 + m^4) \\
2(\Delta + m^2) &> \frac{-1}{(\mu+m)^2}(\Delta - m^2)(\Delta + m^2) \\
2 &< \frac{-(\Delta - m^2)}{(\mu+m)^2}
\end{aligned} \tag{2.25}$$

inserting the value of Δ from (2.10),

$$\begin{aligned}
2(\mu+m)^2 &< -(m^2 - \frac{1}{2}(\omega_p + 2\mu + 2m)^2) + m^2 \\
(2\mu + 2m)^2 &< (\omega_p + 2\mu + 2m)^2
\end{aligned} \tag{2.26}$$

which is clearly satisfied. This shows that ϵ_- evaluated at $\epsilon_2 = \mu + m$ is greater than $\mu + m$, so that the requirement $\epsilon_1 > \epsilon_-$ indeed excludes part of Case 1.

We also show that $\epsilon_- < -\Delta/\epsilon_2$ so that the restriction $\epsilon_1 > \epsilon_-$ does not exclude the entirety of Case 1. Again we show this at the specific value of

$\epsilon_2 = \mu + m.$

$$\begin{aligned}
\epsilon_-\big|_{\epsilon_2=\mu+m} &< \frac{-\Delta}{\mu+m} \\
\frac{-\Delta(\mu+m)}{m^2}\left(1-\sqrt{1-\frac{m^2}{(\mu+m)^2}}\sqrt{1-\frac{m^4}{\Delta^2}}\right) &< \frac{-\Delta}{\mu+m} \\
\left(1-\sqrt{1-\frac{m^2}{(\mu+m)^2}}\sqrt{1-\frac{m^4}{\Delta^2}}\right) &< \frac{m^2}{(\mu+m)^2} \\
\underbrace{\left(1-\frac{m^2}{(\mu+m)^2}\right)}_{>0} &< \sqrt{1-\frac{m^2}{(\mu+m)^2}}\sqrt{1-\frac{m^4}{\Delta^2}} \\
\sqrt{1-\frac{m^2}{(\mu+m)^2}} &< \sqrt{1-\frac{m^4}{\Delta^2}} \\
\left(1-\frac{m^2}{(\mu+m)^2}\right) &< \left(1-\frac{m^4}{\Delta^2}\right) \\
\Delta^2 &> m^2(\mu+m)^2
\end{aligned} \tag{2.27}$$

which is again clearly satisfied (see (2.10)). Thus we see that the requirement that $\epsilon_1 > \epsilon_-$ excludes some part of Case 1, but there remain parts of Case 1 to be included.

Now we wish to find the value of ϵ_2 where ϵ_- crosses $\mu + m$ to determine which region of Case 1 is excluded. We call this value ϵ_2^*. To do this we solve $\epsilon_-(\epsilon_2) = \mu + m$ for ϵ_2. Because ϵ_- is the solution to a quadratic equation, we can exploit a symmetry to get the answer:

$$\epsilon_-(\epsilon_2^*) = \mu + m \leftrightarrow \epsilon_-(\mu + m) = \epsilon_2^*. \tag{2.28}$$

See Figure 2.1 for a graphical representation of the region of integration with all boundaries marked.

To summarize, the plasma frequency and chemical potentials impose the following restriction. The scattering angle is restricted to

$$-1 < \cos\theta_{12} < \frac{-\Delta - \epsilon_1\epsilon_2}{|\vec{p}_1||\vec{p}_2|} \tag{2.29}$$

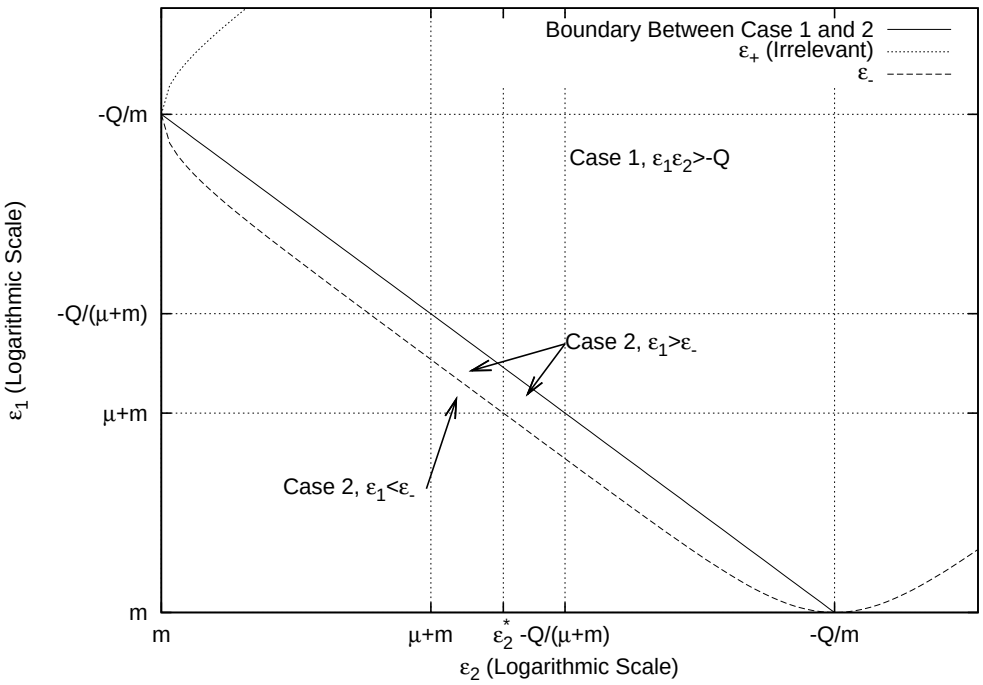

Figure 2.1: Energy phase space for emissivity integral. The region of integration is everything greater than $\mu + m$ on each axis and above ϵ_{-}.

while the energies of the two electrons are restricted to

$$\epsilon_1 > \begin{cases} \epsilon_- & \text{if } \epsilon_2 < \epsilon_2^* \\ \mu + m & \text{if } \epsilon_2 > \epsilon_2^* \end{cases} \tag{2.30}$$

$$\mu + m < \epsilon_2. \tag{2.31}$$

2.3 Phase Space Integral

2.3.1 Angular Integral

Using the expression (2.1) and the restriction (2.11) we can perform the integration over angles. The entire problem is cylindrically symmetric, so the zenith angles each give 2π. There is only one azimuthal angle in the problem: the relative angle between the two incoming electrons θ_{12}. Thus we can change variables from $d\cos\theta_1 d\cos\theta_2$ to $2d\cos\theta_{12}$. We also change from p^2dp to $|\vec{p}|\epsilon d\epsilon$. (2.1) becomes

$$Q = \frac{1}{2}\int\int\int_{\frac{-\Delta-\epsilon_1\epsilon_2}{|\vec{p}_1||\vec{p}_2|}}^{1} 2d\cos\theta_{12}\frac{2\pi|\vec{p}_1|\epsilon_1 d\epsilon_1}{(2\pi)^3}\frac{2\pi|\vec{p}_2|\epsilon_2 d\epsilon_2}{(2\pi)^3}F(\epsilon_1,\epsilon_2,\cos\theta_{12}). \tag{2.32}$$

Because the function F depends on θ_{12}, the angular integration (and the following energy integrations) must be performed numerically.

2.3.2 Energy Integral

The upper limit of integration on ϵ_1 depends on the value of ϵ_2, so the integral must be broken into two parts.

$$\int_{\mu+m}^{\epsilon_2^*}\int_{\epsilon_-}^{\infty}\cdots d\epsilon_1 d\epsilon_2 + \int_{\epsilon_2^*}^{\infty}\int_{\mu+m}^{\infty}\cdots d\epsilon_1 d\epsilon_2 \tag{2.33}$$

2.4 Integrated Cross-Section

In the integral (2.1) there is an expression

$$F(\epsilon_1,\epsilon_2,\cos\theta_{12}) = 2n(\epsilon_1)2n(\epsilon_2)(2\tilde{n}(\mathcal{E}))^2\int_{\omega_p}^{\omega_{max}}\omega\left(\frac{d\sigma}{d\omega}\right)d\omega \tag{2.34}$$

where the first two factors are incoming electron Fermi functions

$$n(\epsilon_i) = \frac{1}{1 + e^{(\epsilon_i - \mu)/T}} \tag{2.35}$$

and $\tilde{n}(\mathcal{E})$ is the effective outgoing electron degeneracy factor described by Eq. (2.38). The factors of 2 account for the two spin states of the electrons.

The photon energy integral is the first moment of the total cross-section. It is integrated from the minimum photon energy (the plasma frequency) to the highest kinematically allowed photon energy $\omega_{max} = \epsilon_i - \frac{m^2}{\epsilon_i}$ where ϵ_i is the energy of incoming electron i.

The differential cross-section $d\sigma$ is taken from [2] and is a slight generalization of a textbook result [5]. It gives the cross-section for emission of a photon with energy $\omega \ll \omega_{max} - m$ from each ultra-relativistic electron in an arbitrary frame of reference. The photons emitted by each electron do not interfere in the ultra-relativistic approximation [5]. This is because each electron only emits in a narrow cone in the direction of its motion, and in the center of mass frame these point in different directions. As mentioned in Section 1.4, the photons whose energies are $\omega_{max} - m < \omega < \omega_{max}$ are not included, but this is a narrow range of energies and the cross-section is smallest in this range (see Figure 1.2). The cross-section is

$$\begin{aligned} d\sigma &= d\sigma^{(1)} + d\sigma^{(2)} \\ &= 4\alpha r_e^2 \frac{d\omega}{\omega} \frac{\epsilon_1 - \omega}{\epsilon_1} \left(\frac{\epsilon_1}{\epsilon_1 - \omega} + \frac{\epsilon_1 - \omega}{\epsilon_1} - \frac{2}{3} \right) \left(\log \frac{2\nu(\epsilon_1 - \omega)}{m^2 \omega} - \frac{1}{2} \right) \\ &\qquad + (1 \leftrightarrow 2) \end{aligned} \tag{2.36}$$

where $d\sigma^{(i)}$ denotes the radiation from the electron labelled i. The two terms are not entirely independent because the quantity $\nu = \epsilon_1 \epsilon_2 - |\vec{p}_1||\vec{p}_2| \cos\theta_{12}$ depends on both $\vec{p}_1$ and $\vec{p}_2$.

The first moment of the cross-section for emission of radiation from electron i is calculated by simple (but tedious) integration

$$\begin{aligned} \int_{\omega_p}^{A} \omega \left(\frac{d\sigma^{(i)}}{d\omega} \right) d\omega = \frac{2\alpha r_e^2}{3\epsilon_i^2} \Bigg(& 6\epsilon_i^3 \ln \frac{\epsilon_i - \omega_p}{\epsilon_i - A} \\ & + (4 \ln \frac{2\nu(\epsilon_i - \omega_p)}{m^2 \omega_p} - 1) \epsilon_i \omega_p (\omega_p - 2\epsilon_i) - \omega_p^3 (2 \ln \frac{2\nu(\epsilon_i - \omega_p)}{m^2 \omega_p} - 1) \\ & + (4 \ln \frac{2\nu(\epsilon_i - A)}{m^2 A} - 1) \epsilon_i A (2\epsilon_i - A) + A^3 (2 \ln \frac{2\nu(\epsilon_i - A)}{m^2 A} - 1) \Bigg) . \end{aligned} \tag{2.37}$$

where $A = \omega_{max} - m$.

The cross-section (2.36) is calculated at zero temperature and in vacuum [2]. This means that the final electron energies were integrated without using inverse Fermi functions to include final state degeneracy. To avoid having to recalculate the whole cross-section, we note that the cross-section itself is slowly varying, so that some non-constant factors may be approximated as constant to allow their removal from inside the integral sign. These factors are the final electron energy inverse Fermi functions. We approximate their contribution by using an effective final state degeneracy factor of

$$\tilde{n}(\mathcal{E}) \equiv 1 - n(\mathcal{E}) = \frac{1}{1 + e^{(\mu - \mathcal{E})/T}} \tag{2.38}$$

for each outgoing electron where

$$\mathcal{E} = \sqrt{|\vec{p}_1||\vec{p}_2|(1 - \cos\theta_{12}) + \frac{m^2}{4}(2 + \frac{|\vec{p}_1|}{|\vec{p}_2|} + \frac{|\vec{p}_2|}{|\vec{p}_1|})} \tag{2.39}$$

is the centre of mass energy.

2.5 Numeric Integration

With the problem stated in (2.32) and the energy constraints in (2.29) ,(2.30), and (2.31), the integral can now be entered into a numerical integration program. The source code is included in Appendix B. It uses standard Numerical Python libraries based on classic optimized FORTRAN subroutines.

3. Results

3.1 Emissivity

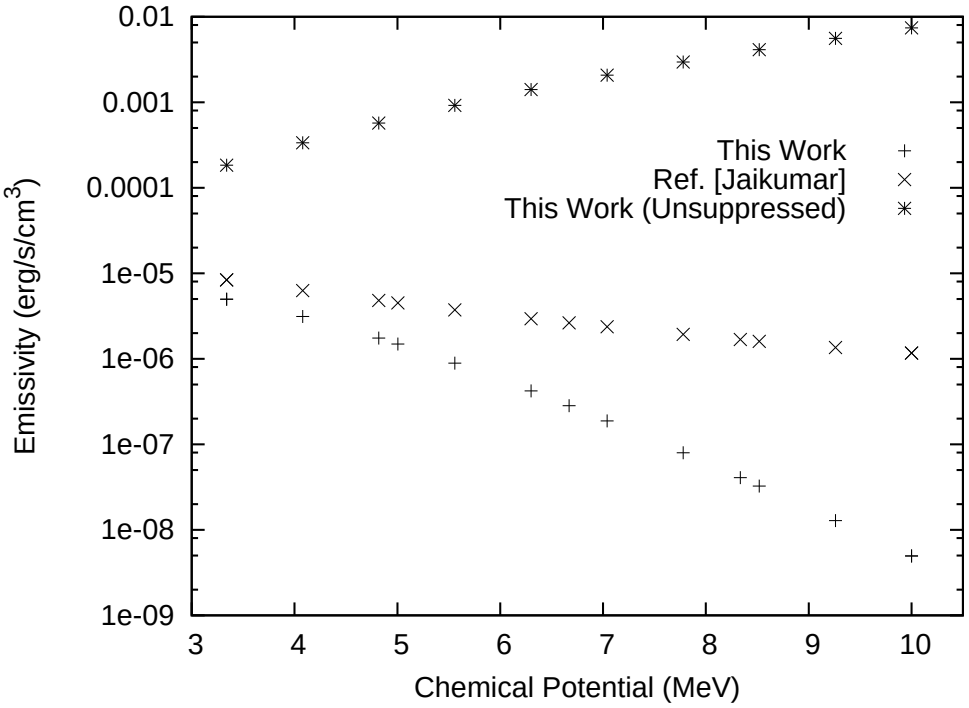

Figure 3.1: Emissivity at 10^{10} K.

The emissivity (Fig. 3.1) is smallest at the edge of the quark star where the chemical potential is highest. We use a typical electron chemical potential here of $\mu_0 = 10\,\mathrm{MeV}$. Towards the outer edge of the electrosphere, the chemical potential drops and the emissivity thus increases from the lifting of the phase space suppression. The "unsuppressed" data points are calculated in the same way, however the electrons were allowed their full phase

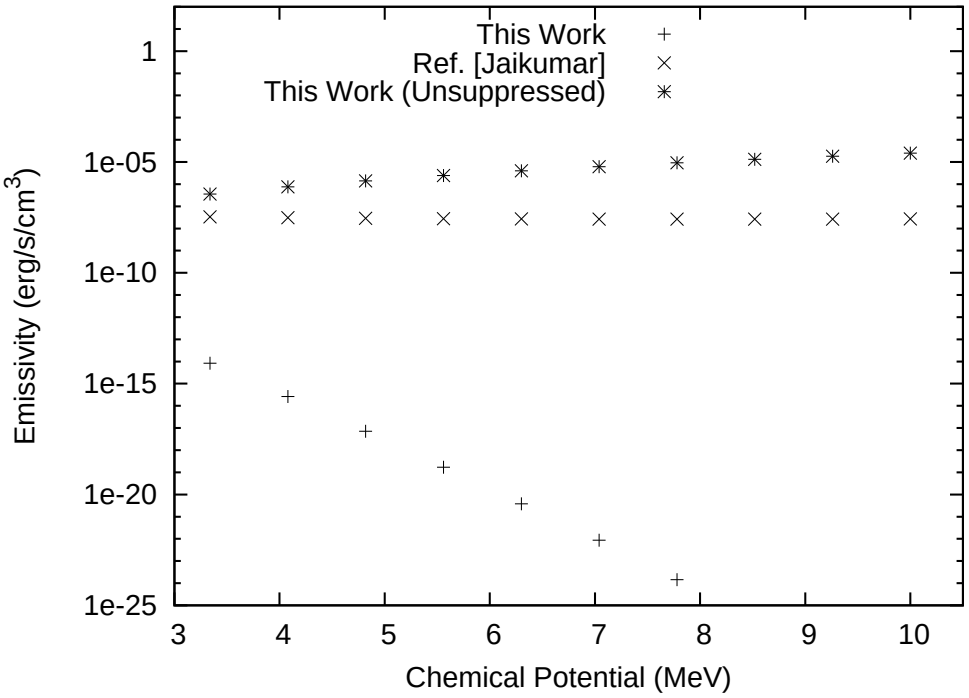

Figure 3.2: Emissivity at 3×10^9 K.

space, neglecting the plasma frequency. Photon energies were still restricted to be above the plasma frequency. These data points are to illustrate the enhancement effect from inclusion of higher energy photons.

At far enough distances, despite the emissivity being unsuppressed, the density is low enough that the emissivity will start decreasing again. This occurs outside of the ultra-relativistic regime where $\mu \lesssim m$, so our calculations do not show this feature. The increase in emissivity with decreasing chemical potential is still present in the previous work, but the effects of the degeneracy were not fully included, so their emissivity is much greater. The result is a severely suppressed emissivity in all regions of the star for typical temperatures $T < 10^{10}$ K due to the phase volume suppression as qualitatively explained in Section 1.4.

The strength of the phase space suppression is dependent on the temperature and is most severe at low temperatures (see Fig. 3.2). At high temperatures, the phase space suppression becomes small enough that the

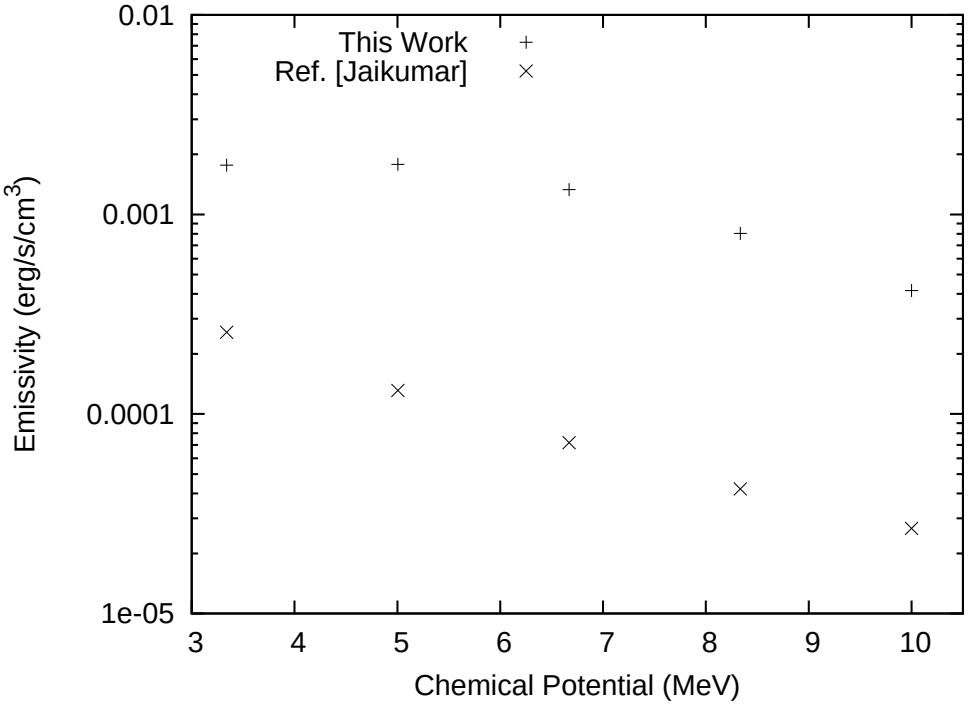

Figure 3.3: Emissivity at 2×10^{10} K.

enhancement from inclusion of higher-energy photons can be seen. In these regions our emissivity is greater than that described in Ref. [17] (see Fig. 3.3).

3.2 Surface Flux

The surface flux of radiation is expressed as the energy radiated per time per surface area of the quark star. We must integrate the emissivity along the radial direction from the bare surface of the quark star ($z = 0$) to infinity. The corresponding computations can be easily done numerically in our framework with any profile function for the chemical potential $\mu(z)$. However, in previous work [17] the authors used a specific profile function to use in their analytical computations. We duplicate their model (see Fig. 1.4) in order to make precise comparisons with their results.

Previous work [17] used an effective boundary of $z_0 \approx 1000\,\text{fm}$. At a large enough distance the chemical potential of electrons will be so low that the electrons will no longer be ultra-relativistic. Including the radiation from this far region is possible in principle because the density profile is known in this regime [12]. As mentioned in Section 3.1, this region is where the density becomes low enough that the overall emissivity starts decreasing with distance, despite the removal of the phase space suppression. Thus the overall emissivity would not be greatly affected by inclusion of this region.

As mentioned in Section 1.1.2, modifications to the electrosphere that extend it to much larger distances than 1000 fm [18] are not considered in this work. In addition to the arguments presented above we should mention that these changes (even if they exist) will not affect the calculated flux at sufficiently large temperatures because the modifications occur in the non-relativistic, low density regime.

In what follows, we assume that the temperature is constant for the entire electrosphere because energy transport is very rapid for dense degenerate matter [10]. The chemical potential profile is that shown in Fig. 1.4. The surface flux is then

$$F = \int_0^{z_0} Q dz. \tag{3.1}$$

For typical temperatures, the suppression is severe to the point of making electron-electron bremsstrahlung negligible compared to electron-positron

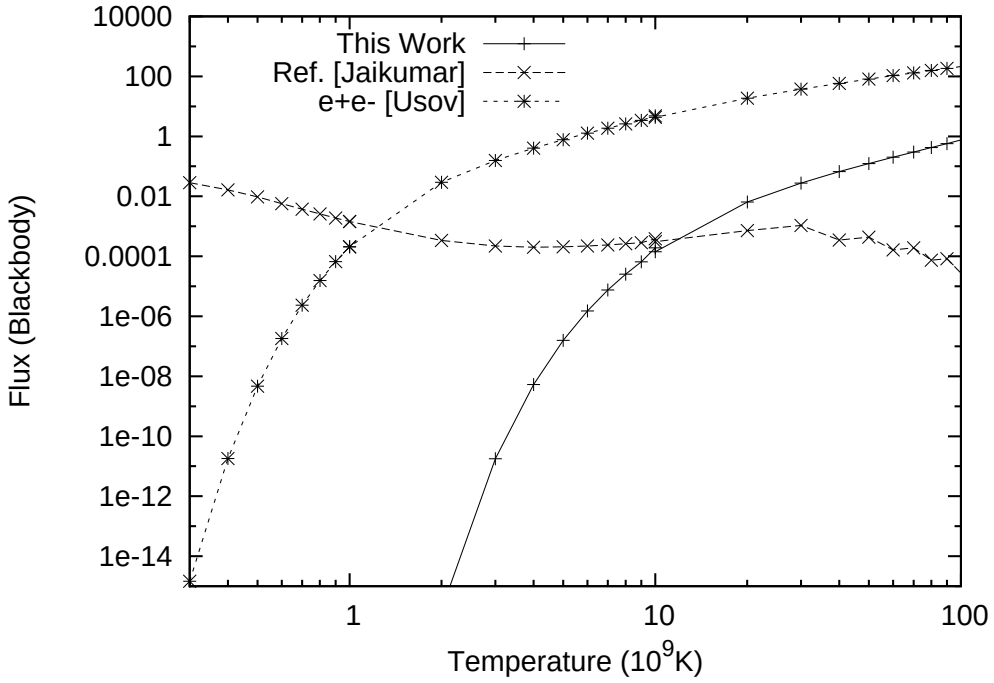

Figure 3.4: Surface flux normalized to blackbody flux. $\mu_0 = 10$ MeV, $z_0 = 1000$ fm. Data points above 10^{10} K are coarsely computed because of slow convergence.

production (see Fig. 3.4). At higher temperatures the suppression lessens, but only well above 10^{10} K. As we mentioned in Section 1.4 the use of the full kinematic phase space results in somewhat higher emissivity than was obtained using Low's theorem in this region. This enhancement however is not strong enough to approach the electron-positron production flux which also increases with temperature. At these high temperatures the dominant radiation mechanism becomes thermal emission [35], so the comparison of electron-electron bremsstrahlung and electron-positron production becomes less relevant.

At much smaller temperatures than we are considering ($T < 10^8$ K) the region of strong degeneracy would extend all the way to the non-relativistic region. The radiation would then come primarily from non-relativistic electrons. In this case the analysis could be performed similarly, using a known profile function which interpolates from the relativistic to non-relativistic regime [11]. The cross-section for such computations also should be modified to include relativistic and non-relativistic regimes along with the ultra-relativistic formula used in the present work. The results of a non-relativistic consideration would also reveal information about the radiative properties of the "strangelet" dark matter candidates [11, 12] which are effectively quark stars with a very small mass.

3.3 Conclusion

The presence of a plasma frequency in the degenerate electron gas in the electrosphere of a bare quark star has many implications on electron-electron bremsstrahlung radiation. The restriction of the electronic phase space beyond the usual degeneracy of the electrons results in a severe suppression of the emissivity at temperatures below a few 10^{10} K.

Full inclusion of photon energies and scattering angles beyond those permitted when using Low's theorem does not significantly increase the emissivity. Consideration of the entire electrosphere including the non-relativistic region would further enhance the emissivity, but it would be a small contribution at sufficiently high temperatures.

The result is that electron-electron bremsstrahlung is a negligible radiation mechanism when compared to electron-positron pair production (with subsequent e^+e^- annihilation) at all temperatures considered. This is contrary to the conclusion found in a previous consideration of the same process

[17]. Electron-positron pair annihilation which results in hard X-ray emission has a very distinct spectrum compared to canonical neutron stars [35]. This could therefore be a powerful tool to establish the existence of quark stars and the strange matter hypothesis.

Bibliography

[1] C. Alcock, E. Farhi, and A. Olinto. Strange stars. ApJ, 310:261–272, November 1986.

[2] Moorad Alexanian. Photon bremsstrahlung from an extreme-relativistic electron gas. Phys. Rev., 165(1):253–257, Jan 1968.

[3] M. G. Alford, K. Rajagopal, S. Reddy, and A. W. Steiner. Stability of strange star crusts and strangelets. Phys. Rev. D, 73(11):114016–+, June 2006.

[4] M. G. Alford, A. Schmitt, K. Rajagopal, and T. Schäfer. Color superconductivity in dense quark matter. Reviews of Modern Physics, 80:1455–1515, October 2008.

[5] V. B. Berestetskii, E. M. Lifshits, and L. P. Pitaevskii. Quantum Electrodynamics, volume 4 of Course of theoretical physics. Oxford Pergamon, 2 edition, 1982. Translation of: Kvantovaya elektrodinamika. Previous ed. published as: Relativistic quantum theory. 1974.

[6] R. Blankenbecler and S. D. Drell. Landau-Pomeranchuk-Migdal effect for finite targets. Phys. Rev. D, 53:6265–6281, June 1996.

[7] A. R. Bodmer. Collapsed nuclei. Phys. Rev. D, 4(6):1601–1606, Sep 1971.

[8] J. Charbonneau and A. R. Zhitnitsky. Topological Currents in Neutron Stars: Kicks, Precession, Toroidal Fields, and Magnetic Helicity. ArXiv e-prints, March 2009.

[9] E. Farhi and R. L. Jaffe. Strange matter. Phys. Rev. D, 30:2379–2390, December 1984.

[10] E. Flowers and N. Itoh. Transport properties of dense matter. II. ApJ, 230:847–858, June 1979.

[11] M. M. Forbes, K. Lawson, and A. R. Zhitnitsky. Macroscopic Relativistic "Nuclei" as dark matter. Application to Diffuse Emission in MeV Band. Preprint, 2009.

[12] Michael McNeil Forbes and A. R. Zhitnitsky. Wmap haze: Directly observing dark matter? Physical Review D (Particles, Fields, Gravitation, and Cosmology), 78(8):083505, 2008.

[13] N. K. Glendenning and F. Weber. Nuclear solid crust on rotating strange quark stars. ApJ, 400:647–658, December 1992.

[14] P. Haensel, B. Paczynski, and P. Amsterdamski. Gamma-ray bursts from colliding strange stars. ApJ, 375:209–215, July 1991.

[15] P. Haensel, J. L. Zdunik, and R. Schaefer. Strange quark stars. åp, 160:121–128, May 1986.

[16] N. Itoh. Hydrostatic Equilibrium of Hypothetical Quark Stars. Progress of Theoretical Physics, 44:291–292, July 1970.

[17] P. Jaikumar, Charles Gale, D. Page, and M. Prakash. Bremsstrahlung photons from the bare surface of a strange quark star. Phys. Rev. D, 70(2):023004, Jul 2004.

[18] P. Jaikumar, S. Reddy, and A. W. Steiner. Strange Star Surface: A Crust with Nuggets. Physical Review Letters, 96(4):041101–+, January 2006.

[19] Ch. Kettner, F. Weber, M. K. Weigel, and N. K. Glendenning. Structure and stability of strange and charm stars at finite temperatures. Phys. Rev. D, 51(4):1440–1457, Feb 1995.

[20] Ch. Kettner, F. Weber, M. K. Weigel, and N. K. Glendenning. Structure and stability of strange and charm stars at finite temperatures. Phys. Rev. D, 51(4):1440–1457, Feb 1995.

[21] D. E. Kharzeev, Larry D. McLerran, and Harmen J. Warringa. The effects of topological charge change in heavy ion collisions: "event by event p and cp violation". Nuclear Physics A, 803:227, 2008.

[22] D. E. Kharzeev and A. R. Zhitnitsky. Charge separation induced by -odd bubbles in QCD matter. Nuclear Physics A, 797:67–79, December 2007.

[23] K. Lawson and A. R. Zhitnitsky. Diffuse cosmic gamma rays at 1 20 MeV: a trace of the dark matter? Journal of Cosmology and Astro-Particle Physics, 1:22, January 2008.

[24] F. E. Low. Bremsstrahlung of very low-energy quanta in elementary particle collisions. Phys. Rev., 110(4):974–977, May 1958.

[25] J. Madsen. Physics and Astrophysics of Strange Quark Matter. In J. Cleymans, H. B. Geyer, and F. G. Scholtz, editors, Hadrons in Dense Matter and Hadrosynthesis, volume 516 of Lecture Notes in Physics, Berlin Springer Verlag, page 162, 1999.

[26] J. Madsen and M. L. Olesen. Boiling of strange-quark matter. Phys. Rev. D, 43:1069–1074, February 1991.

[27] Max A. Metlitski and A. R. Zhitnitsky. Anomalous axion interactions and topological currents in dense matter. Phys. Rev. D, 72(4):045011, Aug 2005.

[28] D. H. Oaknin and A. R. Zhitnitsky. Baryon asymmetry, dark matter, and quantum chromodynamics. Phys. Rev. D, 71(2):023519–+, January 2005.

[29] R. Ouyed, J. Dey, and M. Dey. Quark-Nova. åp, 390:L39–L42, July 2002.

[30] D. Page and V. V. Usov. Thermal evolution and light curves of young bare strange stars. Phys. Rev. Lett., 89(13):131101, Sep 2002.

[31] S. Ratković, S. Iyer Dutta, and M. Prakash. Differential neutrino rates and emissivities from the plasma process in astrophysical systems. Phys. Rev. D, 67(12):123002–+, June 2003.

[32] J. Schwinger. On Gauge Invariance and Vacuum Polarization. Physical Review, 82:664–679, June 1951.

[33] S. L. Shapiro, S. A. Teukolsky, Y. A. Smorodinskij, A. D. Dolgov, and S. N. Rodionov. Black holes, white dwarfs and neutron stars. The physics of compact objects. Wiley, 1985.

[34] V. V. Usov. Bare Quark Matter Surfaces of Strange Stars and e^+e^- Emission. Physical Review Letters, 80:230–233, January 1998.

[35] V. V. Usov. Thermal Emission from Bare Quark Matter Surfaces of Hot Strange Stars. ApJ, 550:L179–L182, April 2001.

[36] E. Witten. Cosmic separation of phases. Phys. Rev. D, 30(2):272–285, Jul 1984.

[37] S. E. Woosley and E. Baron. The collapse of white dwarfs to neutron stars. ApJ, 391:228–235, May 1992.

[38] A. R. Zhitnitsky. Cold dark matter as compact composite objects. Phys. Rev. D, 74(4):043515, August 2006.

Part II

Appendices

A. Notation and Units

In all calculations we use the standard simplification of defining fundamental units to be equal to one. This is not an approximation and no information is lost through doing so, it just makes the math more legible and allows for easy comparison of dimensionality.

$$c = 3.00 \times 10^8 \text{m/s} \equiv 1 \tag{A.1}$$

$$\hbar = 6.58 \times 10^{-16} \text{eVs} \equiv 1 \tag{A.2}$$

$$k = 8.62 \times 10^{-5} \text{eV/K} \equiv 1 \tag{A.3}$$

An electron-volt (eV) is the energy gained by one electron while moved through a potential difference of one volt. It is a common quantity encountered everywhere in physics. The definitions above allow us to express all quantities in terms of powers (or inverse powers) of energy in eV.

For example, to express time (seconds) in energy, we simply rearrange equation (A.2) to solve for seconds. We see that $1\,\text{s} = 1.52 \times 10^{14}\,\text{eV}^{-1}$. Similarly we can express distance in eV^{-1}, energy, momentum, mass, frequency and temperature in eV. Compound units are also expressed in eV, for example volume would be eV^{-3}.

This allows us to directly compare quantities that would otherwise only be related by a constant factor. For example from $E = mc^2$, we can see that mass is really just a type of energy, so the electron's "mass" is 511 keV without bothering with the c^2. Similarly the frequency of a photon has to be converted to energy with $E = \hbar\omega$, but it's easier to just talk about its energy anyways.

At the end of the calculations, we convert back to more conventional units using the same definitions above.

In this problem all bodies are massive and relativistic. This means that all the particles have finite mass, even the photon with an "effective" photon mass. Also all calculations are done considering special relativity. Massive objects in special relativity all follow the relation $\epsilon^2 - \vec{p}^{\,2} = m^2$. From this we see that energy and magnitude of momentum for a given particle are

essentially equivalent. Given an energy, there is only one momentum that corresponds. There will be frequent conversions between the two. Often the particles will be ultra-relativistic. This means that they are moving so close to the speed of light that their energy is much greater than their masses. In this case, their energy and momentum are almost exactly the same $\epsilon \sim |\vec{p}\,|$.

B. Source Code

B.1 Emissivity Integrator

```
"""This code integrates an arbitrary cross-section over t...  ⇒
...wo degenerate fermion momenta.  It assumes high degenerac... ⇒
...y, but not zero temperature.  There is a plasma frequency... ⇒
... as an effective photon mass.  The integral is returned a... ⇒
...s a data file as a function of temperature and chemical p... ⇒
...otential."""

#To run python properly, use the command ipython -pylab f...  ⇒
...rom ~/project01/PYTHON, then run "import project01"

import pylab
from pylab import *

from scipy import integrate, optimize, log, log10

import numpy
from numpy import inf, pi, sqrt, exp, arctan
from numpy import vectorize, linspace, hstack, logspace, ...  ⇒
...append

scale = 1.0
# This is to simplify my scale transformations.  Set it t...  ⇒
...o 1.0 for MeV, 1e3 for keV, 1e6 for eV, etc.
suppression = True
# I can toggle this parameter to "turn off" my plasma fre...  ⇒
...quency in a nice way.
alpha = 1./137.035999679        # Fine structure constant.
m = 0.51099892*scale            # Mass of electron in MeV.
```

```
r = alpha/m                    # Electron radius.
k = scale*8.6173e-11           # Boltzmann constant in Me...          ⇒
...V/K.
small = 1.0
#This is a generic "small" number to use in "much less th...          ⇒
...an" or "much more than" expressions.  A << B is converted...       ⇒
... to A < B*small.

hbarc = 197.3269631e-13; #This is "1" in MeV*cm
hbar = 6.5811899e-22; #This is "1" in MeV*s
conv = 1.60217646e-6; #This is "1" in erg/MeV
ergscm3toMeV5 = hbarc*hbarc*hbarc*hbar/conv
#This converts erg/s/cm^3 to MeV^5.

def final(T,mu):
    def fermi(E):              #A fermi function for use ...          ⇒
...in the integral.  It doesn't break at T=0.
        if T == 0.0:
            if (E-mu)==0.0:
                F = 0.5
            elif (E-mu)>0:
                F = 0.0
            else:
                F = 1.0
        else:
            F = 1./(exp((E-mu)/T)+1.)
        return F
    def antifermi(E):
        if T == 0.0:
            if (E-mu)==0.0:
                F = 0.5
            elif (E-mu)>0:
                F = 1.0
            else:
                F = 0.0
        else:
            F = 1./(exp((mu-E)/T)+1.)
        return F
```

```
    def p(E):
#This returns the relativistic momentum given an energy. ...
... The "if" statement is for numerical ease if m=0.
        if m == 0.0:
            return E
        else:
            return sqrt(E*E-m*m)

    #Omega is the plasma frequency.
    def omega():
#           if suppression is True:
        ohm = sqrt(4.*alpha*mu*mu/(3.*pi) + 4.*alpha*pi*T...
...*T/9.)
#           else:
#               ohm = 0.0
        return ohm

    #Q is just a common bunch of terms in my calculation.
    Q = m*m-(omega()+2.*mu+2.*m)*(omega()+2.*mu+2.*m)

    def freq(E):
#This is the kinematic cutoff to the photon energy.  E is...
... the energy of each photon in the center of mass frame.
        return E-m*m/E


#I would like to use dblquad(f, a, b, g, h) to make this ...
...more elegant (and probably faster, it also gives an actua...
...l estimate of the integration error).  It calculates int(...
...int(f(y,x), y=g(x)..h(x)), x = a..b).

    def crosssectionC(E1,E2):
#This is my cross section times photon energy integrated ...
...over photon energies from plasma frequency omega to the k...
...inematic cutoff.  Remember, I called it crosssection but ...
...it is NOT an actual cross section.  It's the "first momen...
...t" of the cross section.
```

```
        def xintegrand(x):
            def lowomega(Ea,Eb):
#This is from Alexanian 1968, note that I include lowomeg...  ⇒
...a for E1 and for E2 separately.  These correspond to the ...  ⇒
...low-energy photon contributions from each electron which,...  ⇒
... in the ultrarelativistic approximation, do not interfere...  ⇒
....
                def nu():
                    return Ea*Eb-p(Ea)*p(Eb)*x
                def lag(ohm):
                    return log(2.0*nu()*(Ea-ohm)/m/m/ohm)
                A = freq(Ea)-m
                term1 = 6.0*Ea*Ea*Ea*log((Ea-omega())/(Ea...  ⇒
...-A))
                if omega()!=0.0:
                    term2 = (4.0*lag(omega())-1)*(Ea*omeg...  ⇒
...a()*omega()-2.0*Ea*Ea*omega())
                    term3 = -1.0*omega()*omega()*omega()*...  ⇒
...(2*lag(omega())-1)
                term4 = -1.0*(4.0*lag(A)-1)*(Ea*A*A-2.0*E...  ⇒
...a*Ea*A)
                term5 = A*A*A*(2*lag(A)-1)
                if omega()!=0.0:
                    supp = 2.0/3.0*(term1+term2+term3+ter...  ⇒
...m4+term5)/Ea/Ea
                else:
                    supp = 2.0/3.0*(term1+term4+term5)/Ea...  ⇒
.../Ea
#The integrated cross-section contains terms like omega*l...  ⇒
...og(1/omega), so when suppression is False (omega=0), ther...  ⇒
...e is an error.  The limit is zero, so I manually remove t...  ⇒
...hese terms.
                return supp

            def epsilon(E1,E2):
                return sqrt(p(E1)*p(E2)*(1.0-x)/2.0 + m*m...  ⇒
.../4*(2+p(E1)/p(E2)+p(E2)/p(E1)))
            return (lowomega(E1,E2)+lowomega(E2,E1))*anti...  ⇒
```

```
...fermi(epsilon(E1,E2))*antifermi(epsilon(E1,E2))
        xmax = 1.0
        if suppression is True:
            xmin = (-1.0*Q-E1*E2)/(p(E1)*p(E2))
        else:
            xmin = -1.0

        (xdone,xerror) = integrate.quad(xintegrand,xmin,x...                ⇒
...max)

        return alpha*r*r*xdone


    def integrandC(E2,E1):
#This is the function that I have to integrate dE1, dE2. ...                 ⇒
...
#           if suppression is True:
        C = crosssectionC(E1,E2)*E1*p(E1)*E2*p(E2)*fermi(...                ⇒
...E1)*fermi(E2)*0.125/pi/pi/pi/pi
#           else:
#               C = crosssectionC(E1,E2)*E1*E2*p(E1)*p(E2)*f...             ⇒
...ermi(E1)*fermi(E2)*0.25/pi/pi/pi/pi
        return C

    def innerlimitminC(E2):   #An expression for the lowe...                ⇒
...r limit of integration of the inner integral (dE1).
        def E2minus(E2):
            f = -Q*E2/m/m*(1.0-sqrt(1.0-m*m*(1.0/E2/E2+m*...                 ⇒
...m/Q/Q*(1-m*m/E2/E2))))
            return f
        E2star = E2minus(mu+m)
#E2=E2star is when the limits of integration on E1 change...                 ⇒
....
        if (E2 > E2star)or(suppression is False):
            ilmin = mu+m
        else:
            ilmin = E2minus(E2)
        return ilmin
```

```
    innerlimitmaxC = lambda E2:inf
#dblquad seems to want functions for its inner limits, ev...  ⇒
...en if they are constant.  This function is "inf" for all ...  ⇒
...values of E2.
    outerlimitminC = mu+m
    outerlimitmaxC = inf

    (outerdoneC,outererrorC) = integrate.dblquad(integran...  ⇒
...dC,outerlimitminC,outerlimitmaxC,innerlimitminC,innerlimi...  ⇒
...tmaxC) #2D integral, obvious notation.

    if abs(outerdoneC)>abs(outererrorC):
#This prints the numerical result if it non–zero within t...  ⇒
...he estimated numerical error.  The result is recorded to ...  ⇒
...the data file regardless.
        print "Result: ", outerdoneC, "with error ", oute...  ⇒
...rerrorC

    return outerdoneC          #The completed outer inte...  ⇒
...gral, i.e. the final integral.

def jaikumar(T,mu):
#This function replicateds equation 41 in Jaikumar et al....  ⇒
...  It is their analytic estimate for what I am doing.
    muten = mu/10.0/scale      #Their chemical potential...  ⇒
... is expressed in "10 MeV" units.
    Tnine = (T/k)/(1.0e9)      #Their temperature is e...  ⇒
...xpressed in "10^9 K" units.
    err = False
#Note: Their expression is in erg/cm^3/s.  The emissivity...  ⇒
... that I calculate is in MeV^5.  I need to multiply by hba...  ⇒
...rc^3*hbar/conv.
    def piecewise():
#Their expression contains a piecewise–part, but T and mu...  ⇒
... might be chosen so that neither is valid.
        if Tnine/muten < 0.15*small:
            return 0.02*exp(–0.15/Tnine/muten)
        elif(0.15/muten/muten <= Tnine/muten) and (Tnine/...  ⇒
```

```
...muten < 116*small):
            return 0.034*Tnine/muten*(log(2.0)-0.5)
        else:
            err = True
            return 0.0
    if err is False:
        Q = 1.14e42*(1+0.15*muten*muten/(0.3*muten*muten+...        ⇒
...0.26)-1.61*muten*numpy.arctan(0.92/muten))*muten**4.0*(1....     ⇒
...0+pi*pi/256.0*(Tnine*Tnine/muten/muten))**2.0*log(19.6*mu...     ⇒
...ten)*piecewise()*ergscm3toMeV5
    else: Q = "Invalid Parameters in Jaikumar"
#If the parameters were not valid, this string will show ...        ⇒
...up in the data file.
    return Q

def pm(T,mu):
    #This function gives the emissivity of e+e- annihilat...        ⇒
...ion from Usov.



    #This converts erg/s/cm^3 to MeV^5
    muten = mu/10.0/scale
    Tnine = (T/k)/(1.0e9)
    def J(x):
        R = x*x*x*log(1.0+2.0/x)/3/(1.0+0.074*x)**3+pi**5...        ⇒
...*x*x*x*x/6.0/(13.9+x)**4
        return R
    Qpm = 4.52e42*(0.51+0.0862*Tnine)*muten*Tnine*Tnine*T...        ⇒
...nine*(1.0+pi*pi/256.0*(Tnine*Tnine/muten/muten))**2*exp(-...     ⇒
...11.83/Tnine)*J(11.6*muten/Tnine)
    #This Qpm is in erg/s/cm^3, so I convert it to MeV^5 ...        ⇒
...by multiplying hbarc and hbar and conv.
    return Qpm*ergscm3toMeV5



#This sets the range of my plots in T and mu, also the re...        ⇒
...solution in each axis.
```

```
numpointsT = 10
numpointsmu = 10

#I enter the temperature ranges in Kelvin, but my code us...          ⇒
...es MeV, so I use Boltzmann's constant from above.
TKmin = 1e8
TKmax = 1e10
Tmin=TKmin*k
Tmax=TKmax*k
#If I'm an idiot and entered a larger maximum T than mini...          ⇒
...mum:
if Tmax < Tmin:
    Ttemp = Tmax
    Tmax = Tmin
    Tmin = Ttemp

#mumin = 3.339*scale
mumin = 0.0
mumax= 10.0*scale
#Again, this ensures that mumax > mumin.
if mumax < mumin:
    mutemp = mumax
    mumax = mumin
    mumin = mutemp
mupoints = linspace(mumin,mumax,numpointsmu)

Tpoints = linspace(Tmin,Tmax,numpointsT)

print "Temperature values to be used: ",Tpoints
print "Chemical potential values to be used: ",mupoints
print "Plasma frequency suppression is: ",str(suppression...          ⇒
...)

#This writes my data to a gnuplot–readable file called "d...          ⇒
...ata.dat".
FILE = open("data.dat","w")
#This is the header information for the data file.
FILE.writelines(["#Data file for ",str(numpointsT)," and ...          ⇒
```

```
...",str(numpointsmu)," data points in T and mu, respectivel...  ⇒
...y.  Temperatures range from ",str(Tmin)," to ",str(Tmax),...  ⇒
...".  Chemical potential ranges from ",str(mumin)," to ",st...  ⇒
...r(mumax),".  Electron mass is ",str(m),". Scale factor is...  ⇒
... ",str(scale),". Plasma frequency suppression is ",str(su...  ⇒
...ppression),".\n"])
FILE.write("#Result - Temperature - Chemical Potential - ...  ⇒
...Jaikumar Result - e+e- \n")
FILE.close()

#This loop actually initiates each integration, for every...  ⇒
... combination of T and mu specified.  It's basically just ...  ⇒
...formatting, so it looks ugly.

for i in range(0,numpointsT):
    for j in range(0,numpointsmu):
#I open and reclose the file for each data point to avoid...  ⇒
... losing data if the process is interrupted.
        FILE = open("data.dat","a")
        FILE.writelines(array([str(final(Tpoints[i],mupoi...  ⇒
...nts[j])),' ',str(Tpoints[i]),' ',str(mupoints[j]),' ',str...  ⇒
...(jaikumar(Tpoints[i],mupoints[j])),' ',str(pm(Tpoints[i],...  ⇒
...mupoints[j])),'\n']))
        FILE.close()
            print i," ",j
    FILE = open("data.dat","a")
    FILE.writelines(["\n","\n"])
    FILE.close()

#Go into gnuplot and do 'splot "data.dat" using 2:3:1' or...  ⇒
... 'plot "data.dat" using 3:1' for example.
```

B.2 Flux Integrator

```
"""This code converts a regular data file as outputted ...  ⇒
...by projMODN.py into a gnuplot-readable file for graphin...  ⇒
...g fluxes rather than emissivities, as a function of tem...  ⇒
```

```
...perature."""

import array
from scipy import log, log10
import numpy
from numpy import pi, sqrt, exp, append

scale = 1.0
alpha = 1./137.035999679       # Fine structure constan...        ⇒
...t.
m = 0.51099892*scale           # Mass of electron in Me...        ⇒
...V.
r = alpha/m                    # Electron radius.
k = scale*8.6173e-11           # Boltzmann constant in ...        ⇒
...MeV/K.
hbarc = 197.3269631e-13        # This is "1" in MeV*cm
hbar = 6.5811899e-22           # This is "1" in MeV*s
conv = 1.60217646e-6           # This is "1" in erg/MeV
sigma = 5.67e-5                # Stefan-Boltzmann const...        ⇒
...ant in erg/s/cm^2/K^4
ergscm2toMeV5 = hbarc*hbarc*hbar/conv
#This converts from erg/s/cm^2 to MeV^5.


FILE = open("data.dat","r")

lineasread = "#"
while lineasread[0]=="#":
    lineasread = FILE.readline()
line = lineasread.split()
#This loop reads through all lines starting with the co...       ⇒
...mment character #.  The last line to be read is the fir...   ⇒
...st uncommented one.
#split() splits it into an array containing each of the...      ⇒
... space-delimited terms.

#Q = line[0]    Emissivity
#T = line[1]    Temperature
```

```
#mu = line[2]   Chemical potential
#QJ = line[3]   Jaikumar's Emissivity
#Qpm = line[4]  Usov's e+e- emissivity

fluxfile = open("F.dat","w")
fluxfile.write("#Luminosity/Flux of radiation at variou...        ⇒
...s temperatures.  Temperatures are in MeV, flux is in er...   ⇒
...g/s/cm^2.  The integration was performed for chemical p...   ⇒
...otentials from 10 MeV to 3.33 MeV (1000fm).\n")
fluxfile.write("#Temperature - Flux - Jaikumar Flux - e...       ⇒
...+e- Flux  - Blackbody Flux\n")

while True:
    T = float(line[1])
    Q = []
    mu = []
    QJ = []
    Qpm = []
    while lineasread[0]!="\n":
        Q.append(float(line[0]))
        mu.append(float(line[2]))
        QJ.append(float(line[3]))
        Qpm.append(float(line[4]))
        lineasread = FILE.readline()
        line = lineasread.split()
#This loop reads through the first temperature block an...        ⇒
...d reads the emissivity values into Q.
    print "T=",T

    A = []
    AJ = []
    Apm = []
    for i in range(len(Q)):
        A.append(Q[i]/mu[i]/mu[i])
        AJ.append(QJ[i]/mu[i]/mu[i])
        Apm.append(Qpm[i]/mu[i]/mu[i])
    C = sum(A)/len(A)*(max(mu)-min(mu))
    CJ = sum(AJ)/len(AJ)*(max(mu)-min(mu))
```

```
    Cpm = sum(Apm)/len(Apm)*(max(mu)-min(mu))
    H0 = sqrt(3.0*pi/2.0/alpha)
    F = H0*C
    FJ = H0*CJ
    Fpm = H0*Cpm
    Fcomp = F*conv/hbarc/hbarc/hbar
    FcompJ = FJ*conv/hbarc/hbarc/hbar
    Fcomppm = Fpm*conv/hbarc/hbarc/hbar

    print "F=",Fcomp," erg/s/cm^2","FJ=",FcompJ,"Fpm=",...          ⇒
...Fcomppm
    fluxfile.writelines([str(T)," ",str(Fcomp)," ",str(...          ⇒
...FcompJ)," ",str(Fcomppm)," ",str(sigma/k/k/k/k*T*T*T*T)...       ⇒
...,"\n"])

    while lineasread=="\n":
        lineasread = FILE.readline()
#This loop reads past the two blank lines between block...          ⇒
...s.  The last line to be read is the first non-blank lin...       ⇒
...e in the next block.
    line = lineasread.split()

    if lineasread=="":
        break
```